Improved Drone Classification Using Polarimetric Merged-Doppler Images

Byung Kwan Kim, Hyun-Seong Kang, Seongwook Lee, *Member, IEEE*, and Seong-Ook Park, *Senior Member, IEEE*

***Abstract*— We propose a drone classification method for polarimetric radar, based on convolutional neural network (CNN) and image processing methods. The proposed method improves drone classification accuracy when the micro-Doppler signature is very weak by the aspect angle. To utilize received polarimetric signal, we propose a novel image structure for three-channel image classification CNN. To reduce the size of data from four different polarization while securing high classification accuracy, an image processing method and structure are introduced. The data set is prepared for a three type of drone, with a polarimetric Ku-band frequency modulated continuous wave (FMCW) radar system. Proposed method is tested and verified in an anechoic chamber environment for fast evaluation. A famous CNN structure, GoogLeNet, is used to evaluate the effect of the proposed radar preprocessing. The result showed that the proposed method improved the accuracy from 89.9% to 99.8%, compared with single polarized micro-Doppler image. We compared the result from the proposed method with conventional polarimetric radar image structure and achieved similar accuracy while having half of full polarimetric data.**

***Index Terms*— Convolutional neural network (CNN), micro-Doppler signature (MDS), radar signal analysis, radar signal processing.**

I. Introduction

RECENTLY, microdrones are popular for many civil areas such as logistics, hobby, and professional aerial recordings because of technical advance and low price. However, these drones need monitoring and regulation since it may occur dangerous accidents in the air or abused for criminal acts [1]. For this reason, drone detection and classification are required to radar surveillance system. However, the classification is not easy since drones have low radar cross section (RCS), as similar to birds [2].

After Chen *et al.* [3] published micro-Doppler theory, it is widely applied to various radar targets with micromotions for detection, classification, and recognition problems. With micro-Doppler analysis, classifying the drone with the bird becomes possible since the difference between them is significant [2]. However, there is a problem that radar detection and micro-Doppler analysis are affected by the aspect angle, which is between the line of sight of radar and the normal axis of target. When the aspect angle is close to 90°, the RCS becomes minimum and micro-Doppler signature (MDS) vanishes, making detection and classification hard [2], [6]–[9].

To overcome this difficulty, utilizing both time and frequency domain analysis of MDS is presented in [4] and polarimetric signal analysis is shown in [5]. To classify small consumer drones, polarimetric radar has advantages compared with single polarization radar when they have 90° aspect angle [5]. In other radar application area, polarimetric radar can obtain various features from multiple polarized radar signals [6], [8], [10]–[12]. Thus, in this letter, an improved drone classification is proposed using micro-Doppler data from polarimetric radar.

After Kim *et al.* [13] utilized the convolutional neural network (CNN) to classify the MDS, many researches [14]–[16] are presented the high classification accuracy of CNN for Doppler feature-based radar classification problem. These literatures utilized the alpha and omega of CNN, which extracts feature from image structured data. However, by applying proper preprocessing, the accuracy of classification algorithm can be improved [4]. In this letter, we adopt a well-known image signal processing method for radar preprocessing for CNN to reduce total amount of polarimetric data and compress irrelevant information from MDS.

Therefore, we propose a new image structure for radar classification problem, named polarimetric merged-Doppler image (PMDI). The proposed radar image structure emphasizes the periodicity of MDS, represents multipolarization characteristic, and filters out irrelevant information with the same image data size. To evaluate the proposed method, the classification accuracy is compared with Pauli-RGB and Sinclair, which are conventional polarimetric radar image structure.

The rest of this letter is organized as follows. In Section II, the radar experiment setup and method of extracting polarimetric MDS from a radar target is described. Section III introduces the proposed image structure and its classification results with comparison. Finally, Section IV presents our conclusions of this study.

II. Radar Experiment Setup and Signal Processing

A. Drones and FMCW Radar System

In this letter, we defined the target of interest for the classification problem as bird-like drone, three-bladed drone with same rotating direction, and six-bladed drone (hexacopter) with three clockwise and three counterclockwise direction.

Manuscript received May 20, 2020; revised July 3, 2020 and July 14, 2020; accepted July 19, 2020. This work was supported by research fund of Chungnam National University. *(Corresponding author: Byung Kwan Kim.)*

Byung Kwan Kim is with the Department of Radio and Information Communications Engineering, Chungnam National University, Daejeon 34134, South Korea (e-mail: byungkwan.kim@cnu.ac.kr).

Hyun-Seong Kang and Seong-Ook Park are with the Department of Electrical Engineering, Korea Advanced Institute of Science and Technology (KAIST), Daejeon 34141, South Korea (e-mail: kanghs77@kaist.ac.kr; sopark@ee.kaist.ac.kr).

Seongwook Lee is with the School of Electronics and Information Engineering, Korea Aerospace University, Gyeonggi-do 13557, South Korea (e-mail: swl90@kau.ac.kr).

Color versions of one or more of the figures in this letter are available online at http://ieeexplore.ieee.org.

Digital Object Identifier 10.1109/LGRS.2020.3011114

Fig. 1. Appearance of a bird-like drone manufactured by XTIM.

Fig. 2. Appearance of a hexacopter manufactured by HobbyLord.

Because these targets operate with distinct rotation and movement, which determines the MDS from the target. Also, the weight, appearance, and material of the blade also affect the MDS of the drone, as reported in the literatures and conferences [2], [6], [8]. In this letter, we added bird-like drone to investigate the feasibility of proposed method for nonrotating object.

We investigated the MDS from a bird-like drone by bionic bird and a hexacopter by HobbyLord Corporation. Their appearances are presented in Figs. 1 and 2. The laboratory three-bladed drone is presented by removing three motors from hexacopter.

The frequency modulated continuous wave (FMCW) radar hardware setup is mostly the same as previous studies [4], [5]. In summary, the bandwidth of FMCW signal is 150 MHz and its center frequency is 14.1 GHz with 1-W transmitting power. The FMCW waveform is configured as follows. The sweep time is 250-μs and sampling rate is 1 Msps. For one MDS image generation, samples from total 2000 chirp are used, which correspond to 0.5 s. The MDS is obtained by adopting the short-time Fourier transform (STFT). At first, we processed the received FMCW samples into 2-D range-Doppler matrix as described in [17]. After that, we applied discrete-STFT with the following equation [18]:

$$\text{MDS} = X(m,\omega) = \sum x[n] \cdot \omega[\text{n-m}] e^{-j\omega n} \tag{1}$$

where $\omega[n]$ refers the windowing function and $x[n]$ is the Doppler data at certain range bin from range-Doppler matrix. We applied hamming window and overlapping length of 31 samples. After processing discrete-STFT, we applied additional fast Fourier transform (FFT) along time axis of MDS image to (1) to generate the cadence velocity diagram (CVD) image

$$\text{CVD} = \sum X(m,w) \cdot e^{-\frac{j2\pi}{N} kn} \tag{2}$$

$$\text{MDI} = \text{concatenate(MDS, CVD)}. \tag{3}$$

By filtering MDS and CVD image with custom color mapping and concatenating them, we can obtain an MDI image from single polarization. The example of single polarization MDI from the target is presented in Table I.

B. Experiment Setup in Anechoic Chamber

By supposing a drone flying in the air without any other heavy clutters such as building or power transmission tower, the airborne environment will be similar to anechoic chamber with very low transmit power. To evaluate feasibility of the proposed method, we measured the polarimetric radar signal in the anechoic chamber for fast evaluation, with decreased transmit power from 1 to 30 W.

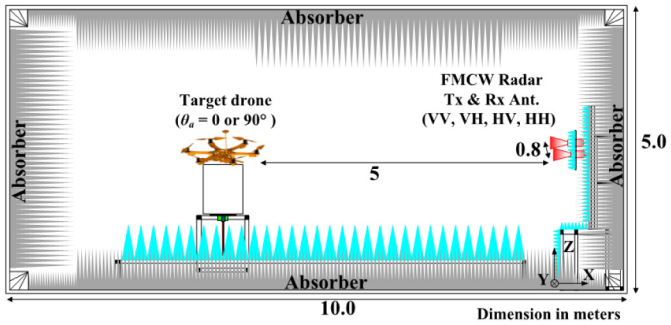

Fig. 3. Measurement setup of micro-Doppler with different aspect angle in the anechoic chamber. Tx and Rx Antenna is separated in *xy* plane. Note that the aspect angle of vertical fixation is 90° and that of horizontal fixation is 0°.

TABLE I

MEASURED MICRO-DOPPLER IMAGE FROM MICRODRONES FOR DIFFERENT POLARIZATION AND ASPECT ANGLE

Polarization (Tx/Rx)		HH	HV	VH	VV
Hexacopter (6p)	Vertical $\theta_a = 90°$	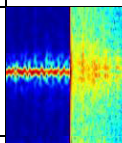	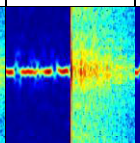	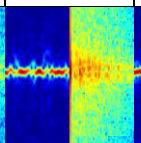	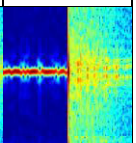
	Horizontal $\theta_a = 0°$	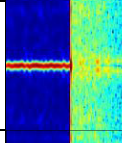	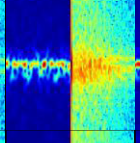	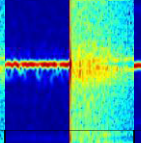	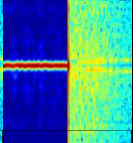
Bird-like Drone	Vertical $\theta_a = 90°$	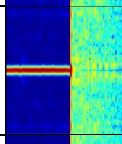	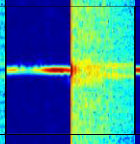	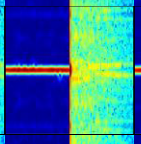	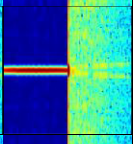
	Horizontal $\theta_a = 0°$	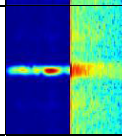	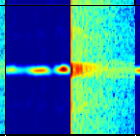	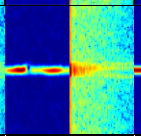	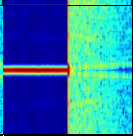

As depicted in Fig. 3, a target is fixed vertically or horizontally to represent both maximum and minimum aspect angle (angle between target and radar line of sight). The transmitting and receiving antenna of radar system is separated by 0.8 m. To obtain enough data, the measurement is repeated by randomly changing target distances 5 $\pm$1 m.

The measured data are processed as described in the previous section. The matrix data are presented as an image for input data set for CNN. In this letter, we used six different image types to compare the drone classification performance: 1) basic MDS [2]; 2) CVD [21]; 3) merged-Doppler image (MDI) [4]; 4) PMDI with Pauli-RGB component (PMDI-Pauli); 5) polarimetric MDI with Sinclair component (PMDI-Sinclair); and 6) polarimetric MDI with 2-D cross correlation (PMDI-xcorr2). The details of image type, generation method, and its physical meaning will be described in Section III-B. The examples of three polarimetric MDIs are presented in Table II.

Fig. 4. Comparison of color mapping between intensity-based image, grayscaled RGB, and Proposed Color mapping.

C. CNN and Radar Data Set

As shown in many literatures, CNN proved its excellent classification performance in radar classification problem [13]–[16]. In some literature, authors proposed novel neural network design and hyperparameter tuning for radar application. However, we first focused on radar data preprocessing because understanding target's characteristic and representing it to data set are also important job for better performance.

Therefore, we used the popular CNN model developed by Szegedy, known as GoogLeNet, inception-v1. The GoogLeNet utilizes inception module with four different types of convolution and pooling operation, which enables higher computational efficiency than AlexNet [14]. The NVIDIA Deep Learning GPU Training System (DIGITS) is employed as neural network implementation. With our heuristic approach, we decided hyperparameters for the network. The learning rate starts from 0.001 with stochastic gradient descent algorithm with batch size of 4. Initialization and other parameters are the same as [14]. Totally, 342 000 images are used in this study for six different image types as described in Section II-B. Each radar image data set consists of 57 000 images, for six classes, which are three different targets with two measurement direction.

Because the data set is smaller than conventional image classification problem, we applied a fourfold cross-validation method [20]. From a total of 57 000 image data sets, 50000 images randomly selected. The classification accuracy for an input image type is obtained by averaging the results for each four-fold. The test set is consisted of a total of 3000 images for six classes.

III. PMDI for Target Classification Using CNN

A. Image Processing Techniques for Polarimetric Data

As shown in [4], the rotation of blade from microdrone produces various MDS in each aspect angle and polarization. Utilizing radar signals from multiple polarization results increases the total amount of data for radar signal processing. In terms of CNN, it is possible to extend channel of network for multiple image or concatenate images from multiple polarization into one image. However, it is not efficient for real-time surveillance since the computational budget will be increased significantly. Therefore, it is required to reduce total data size even if we use multiple polarization radar signal.

In polarimetric SAR image, the Pauli-RGB and Sinclair pseudocolor coding is the most popular method to generate an image from grayscale images from each polarization. To reduce total data size, a colored micro-Doppler image can be converted with grayscale function or certain color channels are utilized like a filtering. Yong *et al.* [22] presented an automatic feature extraction by filtering out red and blue components, since green component represents the frequency and distribution of micro-Doppler. In this literature, we extend this approach into MDS and CVD by varying color mapping scheme.

TABLE II
COLOR CODING SCHEMES OF THREE DIFFERENT PMDIs

Name		Pauli-RGB (PMDI-Pauli)	Sinclair (PMDI-Sinclair)	Cross-correlation (PMDI-xcorr2)
Channel Composition	R	$\lvert HH + VV \rvert$	$\lvert HH \rvert$	$\lvert HH \rvert$
	G	$\lvert HH - VV \rvert$	$\lvert HV \rvert$	$\lvert HV \rvert$
	B	$\lvert HV \rvert$	$\lvert VV \rvert$	$\lvert xcorr2(HH, HV) \rvert$
Output Image		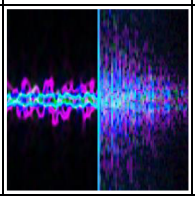	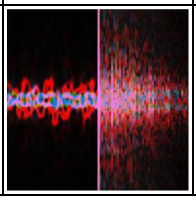	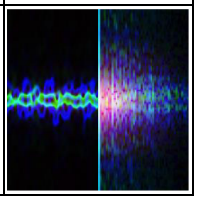

TABLE III
CONVENTIONAL AMPLITUDE-BASED COLOR IMAGE, GRAYSCALED IMAGE, AND PROPOSED COLOR MAPPING SCHEME FOR MDS AND CVD

	Conventional	Grayscaled	Proposed Color Mapping
MDS	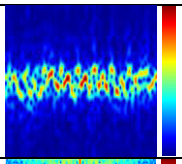	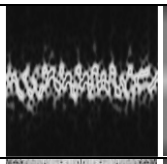	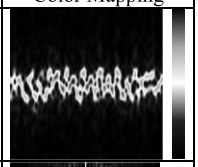
CVD	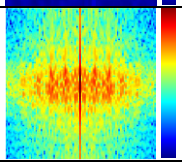	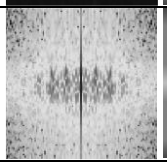	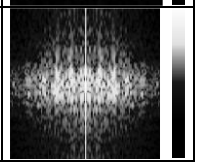

In general image processing, the grayscale function in image processing preserves the shape of image, not the color information, while color represents signal amplitude in micro-Doppler radar image. To preserve both magnitude and shape of MDS in a single channel image, we applied customized color mapping for MDS, and CVD differently, as summarized in Table III.

We propose a custom color mapping for MDI. To preserve shape of micro-Doppler information in MDS area, we filtered out blue image channel, which means low power and noisy signals. In addition, we decreased the values of red component, which means highest magnitude, to represent the micro-Doppler components as a one pattern. On the other hand, in CVD image, we filtered out both blue and green color components, emphasizing red image channel. Because we utilize CVD image to analyze the frequency of micro-Doppler pattern, higher frequency is useful feature for classification.

By this color mapping, the proposed PMDI can represent features of micro-Doppler signal from target better than simple gray-scaled images.

B. Polarimetric Merged-Doppler Image

As described in the previous letter, MDS plots Doppler frequency versus time, and CVD shows the frequency of MDS in Doppler frequency versus frequency of Doppler signal. MDI

TABLE IV
CLASSIFICATION ACCURACY THROUGH FOURFOLD CROSS VALIDATION WITH CNN MODEL, NOTE THAT THE V AND H IN CLASS NOTATION MEAN TARGET FIXATION DIRECTION

Data Type	Image Type	Per-class Accuracy (%)						Total Accuracy (%)
		Bird H ($\theta_a = 0°$)	Bird V ($\theta_a = 90°$)	Drone 3p H ($\theta_a = 0°$)	Drone 6p H ($\theta_a = 0°$)	Drone 3p V ($\theta_a = 90°$)	Drone 6p V ($\theta_a = 90°$)	
Single Polarization	MDS	92.8	**76.8**	96.4	**87.4**	86.4	100	**89.97**
	CVD	92.4	**96.4**	96.8	**83.8**	97.0	98.8	**94.20**
	MDI	98.8	**100**	97.6	**86.0**	98.2	99.4	**96.67**
Multiple Polarization	Pauli-RGB	99.8	**99.6**	100	**99.6**	100	100	**99.83**
	Sinclair	100	**100**	100	**99.8**	97.4	100	**99.53**
	Xcorr2	99.8	**100**	100	**99.8**	99.2	100	**99.50**

represents both time and frequency domain of Doppler signal, and presented its feasibility for micro-Doppler analysis.

In this letter, we extend the MDI images into polarimetric MDI images with three different pseudocolor codings. We compared three different pseudocolor coding schemes to verify feasibility of polarimetric micro-Doppler-based image for classification problem. The coding schemes are summarized in Table II.

We compared the classification performance between two popular and one proposed polarimetric pseudocolor coding scheme: Pauli-RGB [23], Sinclair [23], and cross correlation. The first two schemes are popular in polarimetric synthetic aperture radar (PolSAR) image processing. The conventional pseudocolor coding presents the difference of reflectivity from each polarization in the following ways:

$$\begin{bmatrix} R \\ G \\ B \end{bmatrix}_{\text{Pauli}} = \begin{bmatrix} |\text{HH} + \text{VV}| \\ |\text{HH} - \text{VV}| \\ |\text{HV}| \end{bmatrix}, \quad \begin{bmatrix} R \\ G \\ B \end{bmatrix}_{\text{Sinclair}} = \begin{bmatrix} |\text{HH}| \\ |\text{HV}| \\ |\text{VV}| \end{bmatrix} \tag{4}$$

where Z_{HV} refers radar reflectivity at SAR image with horizontal polarization transmission and vertical polarization receive.

In traditional pseudocolor coding scheme in polarimetric synthetic aperture image (PolSAR), summation or difference between polarizations is widely used because each pixel represents reflectivity of at certain location. However, in micro-Doppler images, a pixel represents intensity of Doppler frequency at a certain time, which is not an absolute value. Considering that micro-Doppler images represent the pattern of Doppler frequency in very short time, approach should be different from PolSAR.

Therefore, we present a pseudocolor coding scheme with 2-D cross correlation for polarimetric micro-Doppler analysis. Because 2-D cross correlation is an effective method in image processing to represent a similarity between two images, utilized as a feature extraction process [24].

In this study, we selected the polarizations for cross correlation operation based on the differences between MDI. By referring results presented in Table I, the VV polarization presents least difference between target classes. On the other hand, the difference between MDI from HH and HV polarization is clear. Therefore, we utilized HH and HV polarization for cross correlation operation in this study. Note that this polarization group can vary with target, by different material, structure, operating frequency of radar. We constructed the cross correlation-based polarimetric-MDI as follows:

$$\begin{bmatrix} R \\ G \\ B \end{bmatrix}_{\text{xcorr2}} = \begin{bmatrix} |\text{HH}| \\ |\text{HV}| \\ |\text{xcorr2}(\text{HH}, \text{HV})| \end{bmatrix}. \tag{5}$$

TABLE V
CONFUSION MATRIX OF BARE MICRO-DOPPLER IMAGE USING GOOGLENET

	Bird H	Bird V	Drone 3p H	Drone 6p H	Drone 3p V	Drone 6p V	Per-class Acc. (%)
Bird H	464	34	1	1			92.8
Bird V	116	384					76.8
Drone 3p H			482	18			96.4
Drone 6p H			63	437			87.4
Drone 3p V					432	68	86.4
Drone 6p V						500	100

C. Classification Results and Discussion

In this section, we carried out the comparison with the classification accuracy results from different micro-Doppler-based image types and summarized in Table IV. By investigating different input image to CNN, we can verify which preprocessing and polarimetric data for deep learning are effective for higher accuracy.

Between single polarized image type results, the classification results showed similar tendency with previous experiments [4], which CVD (94.20%) and MDI (96.67%) result higher accuracy than bare MDS (89.97%), as shown in Table V. On the other hand, accuracy with proposed PMDIs is 99.83% (Pauli), 99.53% (Sinclair), and 99.80% (xcorr2). This high classification accuracy can be verified by analyzing the confusion matrix as presented in Tables V and VI.

Single polarized image commonly showed low accuracies at certain classes, hexacopter with six blades at horizontal fixation (Drone H 6p) and bird-like drone at vertical fixation (Bird V). This case is when the power of returned signal from copolarized signal is very weak, on the other hand, that from cross-polarized signal is a little bit higher, as like reported in [5]. Based on the features and data from additional polarized wave, the proposed PMDIs showed higher accuracy than single polarized ones.

TABLE VI
CONFUSION MATRIX OF PMDI-XCORR2 USING GOOGLENET

	Bird H	Bird V	Drone 3p H	Drone 6p H	Drone 3p V	Drone 6p V	Per-class Acc. (%)
Bird H	499	1					99.8
Bird V		500					100
Drone 3p H			500				100
Drone 6p H			1	499			99.8
Drone 3p V					496	4	99.2
Drone 6p V						500	100

In addition, note that conventional polarimetric pseudocolor coding schemes, Pauli-RGB and Sinclair, can be obtained by using full polarimetric radar (HH, HV, VH, VV). On the other hand, cross correlation pseudocolor coding scheme utilizes only half of polarimetric information, showing similar classification accuracy (99.8%). This means that in drone classification, or classification based on the micro-Doppler-based approach, it can be improved with polarimetry diversity, and it may not require full polarimetry transceiver.

In summary, we achieved high classification accuracy by introducing PMDI. The proposed radar image structure, PMDI, presents the Doppler information in time and frequency domain from multiple polarized radar signal. The CNN successfully classified targets with features from PMDI for different measurement direction and weak returned radar signals.

IV. CONCLUSION

In this letter, we proposed a novel polarimetric radar image processing for drone classification. The PMDI is suggested with polarimetric pseudocolor coding based on modified color mapping for MDS and CVD. To evaluate classification performance of proposed image structure, we measured returned radar signal from hexacopter and bird-like drone. The received full polarimetric radar signal is processed into six different image types (MDS, CVD, MDI, PMDI-Pauli, PMDI-Sinclair, and PMDI-xcorr2) for classification problem.

The polarimetric micro-Doppler-based radar image classification is performed by utilizing CNN structure, GoogLeNet, which proved its performance in image classification. The CNN with basic micro-Doppler image from single polarization data showed 89.97% accuracy; however, our proposed polarimetric methods showed above 99.5%. Also, the cross correlation image structure with half of polarimetric data showed 99.8% accuracy even the radar data are not fully polarimetric.

In conclusion, we have demonstrated that polarimetric MDI can be utilized in the micro-Doppler classification problem for various aspect angle and type of microdrone. With proposed approach, the radar image can represent the features from Doppler in time, frequency, amplitude, and its pattern.

In the future work, we continue on detail analysis on polarimetric MDSs by comparing classification performance between different polarization data group, or other image processing method instead of cross correlation. Also, we will extend micro-Doppler analysis of moving drones, because the drone's blade rotating axis is altered by its moving direction and the Doppler signal from body and blades are mixed together.

REFERENCES

[1] J. Whitehead, "Rise of the drones: Managing the unique risks associated with unmanned aircraft systems," Allianz Global Co. Sp., Munich, Germany, Tech. Rep., 2016. [Online]. Available: https://www.agcs.allianz.com/assets/PDFs/Reports/AGCS_Rise_of_the_drones_report.pdf

[2] M. Ritchie, F. Fioranelli, H. Griffiths, and B. Torvik, "Micro-drone RCS analysis," in *Proc. IEEE Radar Conf.*, Oct. 2015, pp. 452–456.

[3] V. C. Chen, *The Micro-Doppler Effect in Radar*. Norwood, MA, USA: Artech House, 2011.

[4] B. K. Kim, H.-S. Kang, and S.-O. Park, "Drone classification using convolutional neural networks with merged Doppler images," *IEEE Geosci. Remote Sens. Lett.*, vol. 14, no. 1, pp. 38–42, Jan. 2017.

[5] B. K. Kim, H.-S. Kang, and S.-O. Park, "Experimental analysis of small drone polarimetry based on micro-Doppler signature," *IEEE Geosci. Remote Sens. Lett.*, vol. 14, no. 10, pp. 1670–1674, Oct. 2017.

[6] T. Li, B. Wen, Y. Tian, Z. Li, and S. Wang, "Numerical simulation and experimental analysis of small drone rotor blade polarimetry based on RCS and micro-Doppler signature," *IEEE Antennas Wireless Propag. Lett.*, vol. 18, no. 1, pp. 187–191, Jan. 2019.

[7] A. Herschfelt *et al.*, "Consumer-grade drone radar cross-section and micro-Doppler phenomenology," in *Proc. IEEE Radar Conf. (RadarConf)*, May 2017, pp. 0981–0985.

[8] M. Ritchie, F. Fioranelli, H. Griffiths, and B. Torvik, "Monostatic and bistatic radar measurements of birds and micro-drone," in *Proc. IEEE Radar Conf. (RadarConf)*, May 2016, pp. 1–5.

[9] M. Roding *et al.*, "Fully polarimetric wideband RCS measurements for small drones," in *Proc. 11th Eur. Conf. Antennas Propag. (EUCAP)*, Mar. 2017, pp. 3926–3930.

[10] O. A. Krasnov and A. G. Yarovoy, "Polarimetric micro-Doppler characterization of wind turbines," in *Proc. 10th Eur. Conf. Antennas Propag. (EuCAP)*, Apr. 2016, pp. 1–5.

[11] X. Cheng, Y. Chang, B. Rao, J. Liu, and Y. Li, "Joint polarization for micro-Doppler signature enhancement," in *Proc. Eur. Microw. Conf.*, Oct. 2013, pp. 483–486.

[12] L. Jin, W. Qi-Hua, A. Xiao-Feng, and X. Shun-Ping, "Experimental study on full-polarization micro-Doppler of space precession target in microwave anechoic chamber," in *Proc. IEEE Sensor Signal Process. Defense*, Sep. 2016, pp. 1–5.

[13] Y. Kim and T. Moon, "Human detection and activity classification based on micro-Doppler signatures using deep convolutional neural networks," *IEEE Geosci. Remote Sens. Lett.*, vol. 13, no. 1, pp. 8–12, Jan. 2016.

[14] W. Wang *et al.*, "Motion states classification of rotor target based on micro-Doppler features using CNN," in *Proc. IGARSS-IEEE Int. Geosci. Remote Sens. Symp.*, Jul. 2019, pp. 1390–1393.

[15] H. Chen and W. Ye, "Classification of human activity based on radar signal using 1-D convolutional neural network," *IEEE Geosci. Remote Sens. Lett.*, vol. 17, no. 7, pp. 1178–1182, Jul. 2020.

[16] H. Du, T. Jin, Y. Song, and Y. Dai, "Unsupervised adversarial domain adaptation for micro-Doppler based human activity classification," *IEEE Geosci. Remote Sens. Lett.*, vol. 17, no. 1, pp. 62–66, Jan. 2020.

[17] J. Kim, S. Lee, and S.-C. Kim, "Modulation type classification of interference signals in automotive radar systems," *IET Radar, Sonar Navigat.*, vol. 13, no. 6, pp. 944–952, Jun. 2019.

[18] V. Chen, F. Li, S.-S. Ho, and H. Wechsler, "Analysis of micro-Doppler signatures," *IEE Proc. Radar, Sonar Navig.*, vol. 150, no. 4, pp. 271–276, Aug. 2003.

[19] C. Szegedy *et al.*, "Going deeper with convolutions," in *Proc. IEEE Conf. Comput. Vis. Pattern Recognit. (CVPR)*, Boston, MA, USA, Jun. 2015, pp. 1–9.

[20] R. Kohavi, "A study of cross validation and bootstrap for accuracy estimation and model selection," in *Proc. Int. Joint Conf. Artif. Intell.*, 1995, pp. 1137–1145.

[21] S. Björklund, H. Petersson, and G. Hendeby, "Features for micro-Doppler based activity classification," *IET Radar, Sonar Navigat.*, vol. 9, no. 9, pp. 1181–1187, Dec. 2015.

[22] Y. W. Yong, M. N. Hoon, B. J. Woo, K. S. Cheol, and P. J. Hoon, "Automatic feature extraction from jet engine modulation signals based on an image processing method," *IET Radar, Sonar Navigat.*, vol. 9, no. 7, pp. 783–789, Aug. 2015.

[23] J. S. Lee, *Polarimetric Radar Imaging: From Basics to Applications*. Boca Raton, FL, USA: CRC Press, 2009.

[24] K. Briechle and U. D. Hanebeck, "Template matching using fast normalized cross correlation," *Proc. SPIE*, vol. 4387, pp. 95–102, Mar. 2001.